ARTICLES

Cation Spectroscopy and Binding Energy Determination for 1,4-Benzodioxan−Ar_1 and −Ar_2 Complexes

Quanli Gu and J. L. Knee*

Department of Chemistry, Wesleyan University, Middletown, Connecticut 06459

Received: February 27, 2008; Revised Manuscript Received: May 13, 2008

Cation vibronic spectra are measured for 1,4-benzodioxan (BZD) and van der Waals complexes of BZD with one and two Ar atoms using zero electron kinetic energy and mass analyzed threshold ionization spectroscopy. The spectra of the monomer cation were used to measure the frequencies of the two key low-frequency modes which had previously been extensively studied in the neutral S_0 and S_1 states. The aliphatic ring twisting mode, ν_{25}, has an energy of 146 cm^{-1} in the cation, intermediate between the values found in the S_0 and S_1 states. The bending, butterfly-like mode ν_{48} has an energy of 125 cm^{-1}, which is of higher frequency than either of the neutral states. The S_1 spectra of the BZD−Ar_1 and BZD−Ar_2 complexes are recorded and observed to have modest red shifts from the monomer. The cation spectra of the complexes are also measured using mass analyzed threshold ionization spectroscopy including scans at higher energy which are used to determine the Ar binding energies. The energies for the loss of one Ar atom were determined to be 630 ± 10 and 650 ± 10 cm^{-1} for BZD−Ar and BZD−Ar_2, respectively. The similar cation spectra and similar binding energies indicate that each Ar atom in BZD−Ar_2 has a similar binding geometry. Quantum chemical calculations were performed which had fair agreement with the measured binding energies and give some insight into the specific binding geometry.

Introduction

The vibronic spectroscopy of the S_0 and S_1 electronic states of 1,4-benzodioxan (BZD) has recently been characterized in some detail.[1] We have become interested in characterizing the ground electronic state of the cation and also its van der Waals complexes with various species including Ar. Herein, we report on the spectroscopy of the cation and more significantly the binding energy of the Ar_1 and Ar_2 complexes in the cation, the neutral excited state S_1, and the ground state S_0. Recently, we have measured the binding energy for aniline$^+$−Ar and aniline$^+$−Ar_2 cations and found an anomalous value for the dissociation of one Ar atom from the aniline$^+$−Ar_2 system.[2] Measurements on BZD−Ar_2 provide an opportunity to compare the dissociation in a similar system.

Weakly bound molecules have been the subject of intense interest for many years, including studies on structure, rotational, vibrational and electronic spectroscopy, as well as dynamics. Often times, one of the least well defined quantities is the binding energy, which is an important parameter for characterizing the complex. This disparity is due to the fact that most spectroscopic methods probe near the minimum of the bound potential and do not directly probe the dissociation threshold. The primary tools for probing the dissociation threshold are different varieties of action spectroscopy in which vibrational bands are scanned while looking for the onset of dissociation. This can be done on the electronic ground state with IR excitation or stimulated emission pumping,[3–5] in excited electronic states using vibronic excitation,[6,7] or in the cation using either photoelectron spectroscopy[2,8–13] or IR photodissociation.[14–17] In this work, we apply mass resolved threshold ionization (MATI),[10–13,18–21] which is a photoelectron spectroscopy technique to measure the complex binding energies in the cation which can then be accurately transformed to neutral-state binding energies using measured spectroscopic shifts.

For many aromatic molecules, the primary binding site for Ar atoms is the π-system. Often, the Ar atom sits quite close to the center, or depending on substituents, it can be displaced significantly from the center, but still above the plane of the molecule. For molecules with two bound Ar atoms, often the most stable conformation is one Ar atom on either side of the aromatic plane. This sandwich-type geometry can be identified in experimentally observed electronic spectra from the additivity of the spectral shifts going from zero to one to two Ar atoms. The nearly equivalent Ar positions lead to equal spectral shifts. This has been characterized often in S_0 to S_1 spectra[6,22–24] but also in photoelectron spectra in the shifts from S_0 to the cation ground state, D_0^+, or similarly in the S_1 to D_0^+ transitions.[2,8,21,25] While the π-bound geometry for these aromatic−Ar molecules is common, there is the possibility for other binding sites in either the neutral or cation complexes. In recent work, starting with the aniline−Ar_2 complex, we determined that the aniline−Ar π-bound structure was not the minimum in the cation complex.[2] Our experiments did not have structural information on what the actual minimum was, but other recent experimental[16] studies indicate that it is a hydrogen-bonded species. Part of our motivation in studying BZD−Ar_1

* To whom correspondence should be addressed. E-mail: jknee@wesleyan.edu.

10.1021/jp801716p CCC: $40.75
Published on Web 07/09/2008

and BZD−Ar_2 is to see if the global minimum in the cation is the π-bound geometry as expected for the neutral molecule.

Experimental Section

BZD and the complexes BZD−Ar and BZD−Ar_2 have been studied using resonant enhanced multiphoton ionization (REMPI), zero electron kinetic energy (ZEKE) photoelectron spectroscopy, and mass analyzed threshold ionization spectroscopy (MATI). The S_1 spectrum for the monomer is in agreement with the more detailed previous published spectra.[1] To the best of our knowledge, the S_1 spectra of the Ar complexes has not been previously reported. The ZEKE and MATI photoelectron spectra of the monomer and complexes are reported for the first time. The following briefly describes the experimental apparatus, which is presented more completely in several other publications.[2,21,26–28]

The sample was obtained from Aldrich and used without further purification. It was heated to 50 °C in the sample container of a pulsed nozzle (General Valve). This nozzle, located in a differentially pumped molecular beam apparatus, produces a supersonic expansion using He/Ar mixture buffer gas at a total pressure of 2 bar with the percentage of argon in the mixture typically 10%. The resulting molecular beam is skimmed before entering the second chamber, where REMPI, ZEKE, and MATI spectroscopy take place.

Two independently tunable ultraviolet laser pulses are used in the experiments. One laser is a pulsed nanosecond Nd:YAG device operating at 20 Hz (Lumonics NY-61) pumping a tunable dye laser (Lumonics HD500) with a visible bandwidth of 0.05 cm^{-1}. The visible output of this laser is frequency doubled (Spectra-Physics WEX) and provides approximately 1 mJ per pulse in the UV range. The second laser system is also a Nd:YAG device (Quanta-Ray GCR-3) pumping a tunable dye laser (Quanta-Ray PDL) equipped with frequency doubling capabilities (Spectra-Physics WEX). These two lasers are spatially overlapped in the interaction region, one functioning as the pump laser and the other as the probe. The temporal overlap of the lasers is controlled by a digital pulse generator (Stanford Research Systems, DG535) and adjusted to optimize the two-color dependent signal.

REMPI spectra were acquired using a single laser providing both the excitation and ionization photons. The ZEKE and MATI spectra were obtained by fixing the pump to a desired resonance in S_1 and scanning the probe through the spectral region of the ionization potential. For MATI spectra, the pump and probe excitation occurs in a field-free environment, and then, following a delay of around 0.1 μs, a small discrimination voltage (+ 1 V/cm) is used[29] to separate any prompt ions from high Rydberg states which may have been created. Under the influence of this discrimination field and given sufficient time (~20 μs), a pulse sequence achieving the Wiley−McLaren[30] ion space focusing was applied to field ionize the remaining highly excited Rydberg states in the interaction region and direct the resulting ions to the detector. The large voltages used in the field ionization (~1000 V/cm) lead to a broadening of the cation vibronic peaks to approximately 7 cm^{-1} fwhm. Further details of the MATI apparatus are given in a recent publication.[2] ZEKE spectra were collected in a similar fashion but with small extraction voltages of approximately 100 V/cm. This results in measured linewidths of approximately 5 cm^{-1}.

Data collection is performed using digital capture of the ion arrival signal (HP 54510A oscilloscope). After signal averaging for eight laser shots, the oscilloscope data is transferred by GPIB to a PC and the entire mass spectrum is stored as a function of wavelength. The laser wavelength scans are computer controlled, and the resulting specta in the appropriate mass channels are constructed from the full data set.

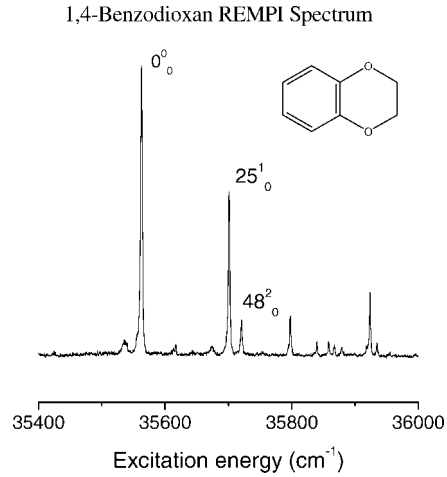

Figure 1. Mass resolved MPI spectra for the S_1 origin region of BZD. The mass-gated spectra were obtained by scanning the pump laser as indicated and probing with a fixed laser energy which exceeded the ionization potential. The assignments for the origin and two key vibronic transitions are indicated.

Results and Discussion

A. 1,4-Benzodioxan Monomer. Figure 1 shows the S_1 spectra of BZD in the region of the electronic origin at 35564 cm^{-1}. This was obtained using two-color photoionization where the probe laser frequency was fixed above the ionization threshold and the pump laser was scanned. The spectrum is in agreement with recently published results,[1] and thus only a small portion of the spectrum was scanned. There are three features to note in the spectrum, the electronic origin at 35564 cm^{-1} and the two vibrational bands assigned as 25^1_0 at 139 cm^{-1} excess energy and the relatively weak 48^2_0 band at 157 cm^{-1}. These two bands correspond to the bending (ν_{48}) and twisting (ν_{25}) of the oxygen-containing aliphatic ring relative to the planar phenyl component. A potential for these coupled motions was constructed by Yang et al.[1] by fitting the observed frequencies and intensities of the vibrational progressions in the S_0 and S_1 electronic states.

Given the interest in these modes, we have pursued their measurement in the cation ground state as well. To do this we have measured the photoelectron spectrum using the ZEKE technique and pumping through the S_1 electronic origin as well as the S_1 25^1_0 and 25^2_0 bands and the 48^2_0 and 48^4_0 bands. These spectra are shown in Figure 2, with the energy scale relative to the monomer ionization potential determined to be 63829 cm^{-1}. A summary of the cation vibrational frequencies extracted from these spectra is given in Table 1. Also included are the calculated vibrational frequencies, which are described more fully below.

In the cation, the ν_{25} twisting mode takes on a value intermediate between the ground-state and S_1 values, which is quite typical since one is taking a π electron, exciting it to an antibonding orbital, and then removing the antibonding electron upon ionization. What is a bit surprising, as shown in the calculations, is that the C−O bonds decrease in length significantly, going from 1.37 Å in the neutral ground state to 1.31 Å in the cation. The O−C−C−O dihedral angle also undergoes a change from an approximately planar 0° angle in the neutral state to a noticeably nonplanar 7° in the cation state. One might expect that this would create a double well potential with a resulting dramatic change in the twisting vibrational mode.

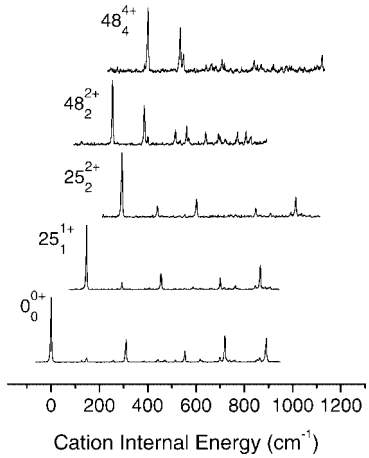

Figure 2. ZEKE spectra of the BZD monomer obtained by pumping the S_1 vibronic bands as indicated and scanning the probe above the ionization potential. The energy scale is relative to the ionization threshold at 63829 cm^{-1}.

However, as the calculations show and as previously demonstrated for a similar situation in 9,10-dihdrophenanthrene,[31,32] the twisting normal mode of ν_{25} does not carry the molecule through the planar configuration and so is not described by a double well potential. The C−O bond shortening and distortion to a nonplanar position of the oxygens apparently does make the unsaturated portion of the molecule stiffer with regard to out-of-plane bending, and so mode ν_{48} increases in frequency to 125 cm^{-1}, greater than the values in either the S_0 or S_1 states.

B. 1,4-Benzodioxan−Ar_1 and −Ar_2 Complexes. Figure 3 shows the S_1 spectrum in the origin region gating on the corresponding mass of the BZD−Ar_1 and BZD−Ar_2 complexes with the monomer shown for reference. An important point to note is the shift of the BZD−Ar and BZD−Ar_2 origin bands, 62 and 122 cm^{-1}, respectively, from those of the monomer, showing additivity of the S_1 shifts.

The MATI spectra are obtained by pumping through the respective origins of each complex and scanning the probe laser above the ionization potential and gating on the mass channels of interest. Figure 4 shows the MATI spectrum of each complex near the ionization threshold. The shifts of the BZD^+−Ar and BZD^+−Ar_2 cation origin bands from the monomer show a high degree of additivity with values of 151 and 302 cm^{-1}, respectively. Combining these shifts with the S_1 band shifts yields the values for the change of the total ionization potentials of the complexes relative to the neutral ground state and these are 213 and 424 cm^{-1} for the Ar_1 and Ar_2 species.

The MATI spectrum for each complex shows a vibronic pattern with one pronounced progression in a low-frequency mode which is presumably due to an intermolecular vibration. These patterns, for both the BZD^+−Ar and BZD^+−Ar_2 complexes, are quite similar to those observed and assigned in aniline$^+$−Ar_1 and −Ar_2 as the symmetric bending vibration. In BZD^+−Ar the first member has a frequency of 27 cm^{-1}, and in BZD^+−Ar_2 the frequency is 20 cm^{-1}. By analogy with the aniline case and our calculations below, we assign this vibration as a bending motion along the long C_2 axis of the molecule. The vibronic activity upon ionization likely results from the slight displacement of the Ar atom toward the oxygen atoms that, along with the tighter bond in the cation, gives rise to the Franck−Condon progression. This geometry change is shown below in the calculations of the neutral and cation complex structures. The more pronounced progression in the BZD^+−Ar_2 complex results from a similar effect and is almost identical to the activity seen in aniline$^+$−Ar_2.

At the ionization threshold the MATI signal appears completely in the parent channel, with no dissociation detected. As the MATI probe is scanned to higher energy signal, the signal is eventually observed in the channel of the dissociation product (BZD^+ for the BZD^+−Ar complex and BZD^+−Ar for BZD^+−Ar_2). The appearance of the dissociation product then marks the dissociation threshold and can be used to measure the cation complex binding energy. This technique has been well documented by Neusser et al.[10,11]

B1. 1,4-Benzodioxan$^+$−Ar → 1,4-Benzodioxan$^+$ + Ar. Figure 5 shows the MATI spectrum of the BZD^+−Ar_1 cation complex at higher energy, again pumping through the S_1 origin, and plotting signals for both the complex (BZD−Ar^+) channel and the monomer (BZD^+) channel (the product is shown as a negative spectrum so as to be clearly identified compared to the reactant). The x axis indicates the total energy above the complex ionization threshold for BZD−Ar (28117 cm^{-1}) and thus directly represents the total vibrational energy available in the complex. The point at which the complex mass signal disappears is between 625 and 640 cm^{-1}. It should be noted that immediately below 625 cm^{-1} a signal is observed in both the reactant and product channels. This was observed and explained by Neusser et al.[33] and is due to Rydberg state coupling and the large voltage extraction pulses used. The threshold for disappearance of the complex signal is not affected by the field and thus is used as a more reliable value to determine the dissociation energy. In this particular case, it appears as if the signal disappears at 625 cm^{-1}; however, the overall signal level in this region is quite small (as evidenced by small signal in the product channel) and so the range of uncertainty of dissociation extents to ∼640 cm^{-1} where the product signal picks up with no observable reactant signal. Therefore, the BZD^+−Ar dissociation energy is determined to be 630 ± 10 cm^{-1}. Further evidence that the monomer ion signal originates from the complex is given by the appearance of the spectral features at 700 cm^{-1} in the figure. These bands have the characteristic pattern associated with the BZD^+−Ar MATI spectrum (Figure 3) and thus confirm the parentage. The binding energy in the S_1 and S_0 neutral states can be obtained by combining this cation binding energy with the measured spectral shifts. This results in values of 485 ± 10 cm^{-1} for S_1 and 420 ± 10 cm^{-1} for S_0. The uncertainty in the spectroscopy shifts is quite small compared with the uncertainty of the MATI dissociation threshold.

One point to emphasize is that after laser excitation there is a ∼25 μs delay until the extraction pulse is applied. Thus, it is unlikely that metastable complexes would give an artificially high dissociation threshold. This is always a concern in S_1 excited-state measurements where the short excited-state lifetime might prevent the true threshold from being observed.

B2. 1,4-Benzodioxan$^+$−Ar_2 → 1,4-Benzodioxan$^+$−Ar + Ar. Figure 6 also shows the MATI spectrum of the BZD−Ar_2 complex at higher energy in the cation, again pumping through the S_1 origin, and plotting signal for both the complex (BZD^+−Ar_2) parent channel and the expected product channel (BZD^+−Ar). The onset for dissociation is quite clear in this case as indicated by the arrow in the figure, yielding a dissociation energy of 650 ± 10 cm^{-1}. Again, the product signal appears before complete loss of the parent, but we use the disappearance of the reactants as the precise dissociation threshold. This results in values of 497 ± 10 cm^{-1} for S_1 and 437 ± 10 cm^{-1} for S_0.

The value for the dissociation energy for BZD^+−Ar_2, 650 cm^{-1}, is 20 cm^{-1} greater than that for the loss of Ar in

TABLE 1: ν_{25} and ν_{48} Vibrations in Three Electronic States

	S_0 (cm^{-1})		S_1 (cm^{-1})		D^+_0 (cm^{-1})	
vibration	experiment[a]	calculation[b]	experiment[a]	calculation[c]	experiment	calculation[b]
ν_{25}	166	160	140	142	146	142
ν_{48}	104	102	80	102	125	122

[a] Values obtained in ref 1. [b] Calculated using DFT B3LYP with aug-cc-pVDZ basis set and scaled by 0.95. [c] Calculated using RCIS aug-cc-pVDZ basis set and scaled by 0.90.

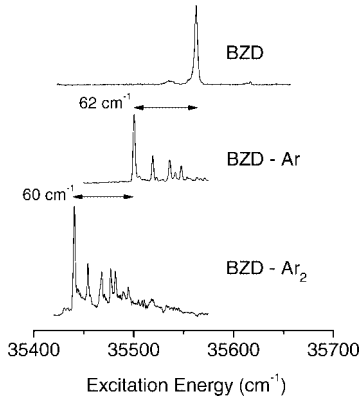

Figure 3. Mass resolved MPI spectra for the S_1 origin region of BZD, BZD−Ar, and BZD−Ar_2. The mass-gated spectra were obtained by scanning the pump laser as indicated and probing with a fixed laser energy which exceeds the ionization potential by a small amount so as to prevent fragmentation. The shifts of the respective origins are indicated and show additivity for the second Ar atom.

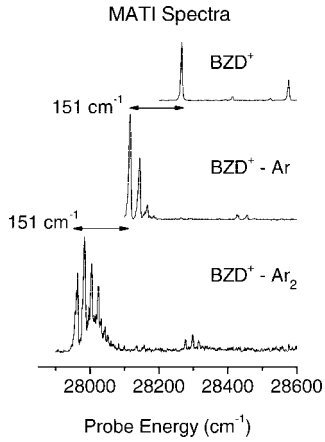

Figure 4. MATI spectra in the region of the ionization threshold for BZD, BZD−Ar, and BZD−Ar_2. The spectra were obtained by pumping the respective S_1 origins and scanning the probe as indicated. The shifts in probe energy, relative to the monomer, are indicated.

BZD^+−Ar, but quite close to being equal within the experimental error ranges. The similar binding energies for each argon atom suggest that their geometry is similar to that of the monomer. There is strong spectral evidence that this is the case. As mentioned above, the spectral shifts from S_0 to S_1 are additive for each of the argon atoms. The additivity is also present in the shifts from S_1 to the cation, being 151 and 302 cm^{-1}, respectively. Although additivity rules have long been identified as an indication of similar binding sites,[6,22–24] there have not been many studies which have directly measured the binding energy of a second Ar atom in a complex.[2,6,8] In one such study on a neutral *p*-difluorobenzene−Ar_2 complex, it was shown that the two π-bound Ar atoms had almost identical binding energies with very small three-body effects.[6] Our measurements on BZD show a similar result, although it does appear that the second Ar atom is slightly more tightly bound.

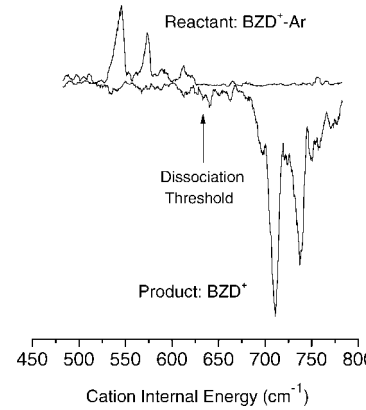

Figure 5. MATI spectra obtained by pumping the BZD−Ar S_1 origin at 35500.7 cm^{-1} and then scanning the probe above the ionization threshold as indicated. The *x* axis is relative to the ionization threshold of this complex at 63616 cm^{-1}. The positive spectrum is the signal obtained by gating on the reactant BZD^+−Ar mass, and the negative spectrum is the signal gating on the dissociation product BZD^+.

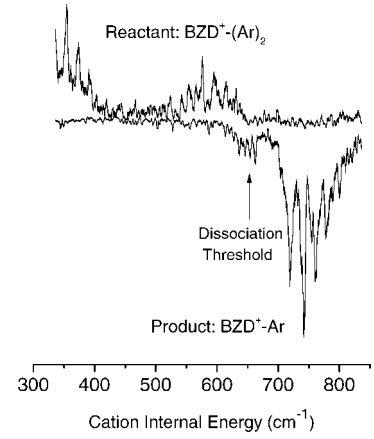

Figure 6. MATI spectra obtained by pumping the BZD−Ar_2 S_1 origin at 35440.8 cm^{-1} and then scanning the probe above the ionization threshold as indicated. The *x* axis is relative to the ionization threshold of this complex at 63405 cm^{-1}. The positive spectrum is the signal obtained by gating on the reactant BZD^+−Ar_2 mass, and the negative spectrum is the signal gating on the dissociation product BZD^+−Ar.

C. Calculations. The accurate calculation of the structure, vibrational frequencies, binding energies, and other properties of van der Waals molecules is now possible with current quantum chemical calculations. However, these calculations are by no means routine, and it has been shown that extensive calculations with large basis sets are required to get the accuracy needed for detailed comparison to experiments.[34–36] The binding energies in particular are difficult to obtain.[34,36,37] The preferred approach for such calculations is the CCSD(T) method with a large correlation consistent basis set such as aug-cc-pVTZ.[34,36] We do not have the computational resources for such calculations but have pursued a slightly lower level approach which is expected to give reasonable geometries and estimates of the bonding energies. We have only pursued calculations on the

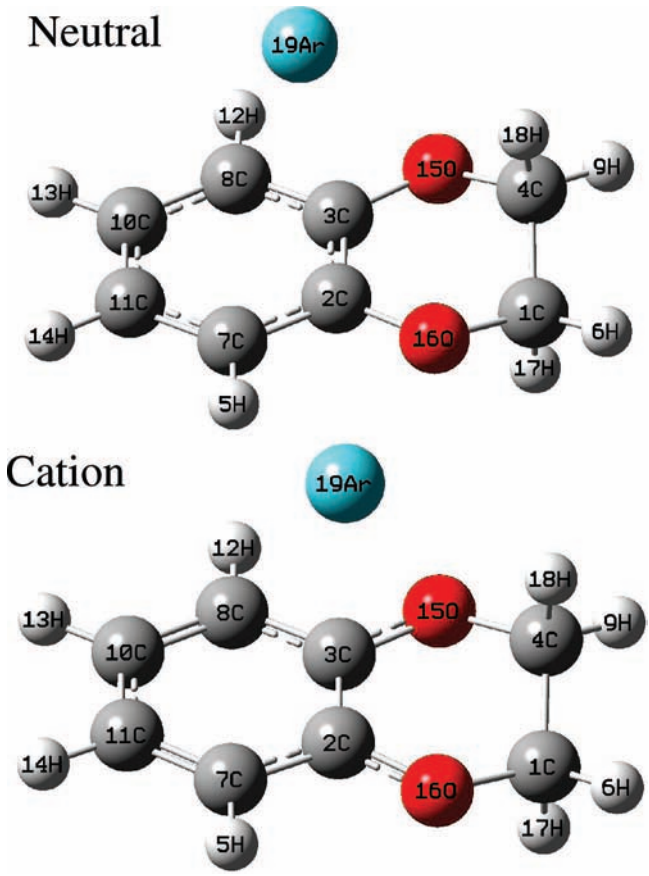

Figure 7. Calculated structure of the neutral and cation BZD−Ar complexes. Note that upon ionization the Ar atom moves noticeably closer to the oxygen atoms. With a view from above, the Ar atom is symmetrically positioned along the short axis of the molecule in both the cation and neutral structures.

Ar_1 complex since experimentally both Ar atoms appear to have equivalent bonding positions.

All calculations were performed using the *Gaussian 03* program.[38] The monomer neutral and cation structure and vibrational frequencies were calculated using density functional theory (DFT) using the B3LYP functional and the aug-cc-pVDZ basis set. The vibrational frequencies and structural changes of interest that occur upon ionization were discussed above and so will not be further addressed here.

The structure and energy of the BZD−Ar neutral and cation complexes were calculated by optimization using the MP2 method and the aug-cc-pVDZ basis set and then doing a single point calculation with the aug-cc-pVTZ basis set and counterpoise correction. For the cation, spin contamination is an issue so the restricted open-shell, ROMP2, method was used. The geometry optimizations for the complexes were performed with a fixed monomer geometry which has been shown to be a reasonable approximation and leads to a more rapid convergence. For the purpose of zero-point energy calculations, the vibrational frequencies of the complexes were calculated, again fixing the BZD monomer and so only determining the intermolecular modes. This is also an approximation but is likely to capture most of the contribution to the loss of zero-point energy during dissociation. Figure 7 shows a picture of the neutral and cation BZD−Ar calculated structures. As expected, the minimum structure has the Ar atom in a π-bound geometry above the phenyl ring. However, it is a bit surprising the degree to which the Ar atom is moved toward the oxygen atoms, particularly in the cation. The cation structure essentially has the Ar located directly above the C−C bond where the oxygen atoms are attached. The calculated binding energy, D_e, for the neutral complex is 596 cm^{-1} and coupled with a zero-point energy correction of 51 cm^{-1} yields a value of 545 cm^{-1} for D_0 as compared with the measured value of 420 cm^{-1}. The calculated value of D_e for the cation is 804 cm^{-1} and with a zero-point energy of 54 cm^{-1} gives a calculated D_0 value of 750 cm^{-1} as compared with the measured value of 630 cm^{-1}. The calculations overestimate the binding energy, but interestingly, they represent the difference between the neutral and cation complexes quite well. Again, this points out the need to go to higher levels of calculation to get the binding energies correct, part of which is likely due to the approximation of the zero-point energy.

TABLE 2: Summary of Representative Aromatic−Ar Binding Energies

molecule	S_0 (cm^{-1})	S_1 (cm^{-1})	cation (cm^{-1})
BZD[a]	417	479	630
aniline[2]	380	440	495
fluorobenzene[8,33]	346	368	568
indole[40]	452	478	537
phenol[41]	364	397	535
dibenzofuran[39]	521	566	636
dibenzo-*p*-dioxin[39]	527	576	739

[a] Values measured in this work.

A directed search for other possible structural minima was performed, and only one additional structure was found. This structure had the Ar atom in the phenyl plane between the H atom attached to the phenyl group and the oxygen atom, but with an energy approximately 400 cm^{-1} above the global minimum π-bound structure, making it just barely bound. It is unlikely that this structure would have any significant intensity in the experimental spectra.

D. Comparison to Other Ar−Aromatic van der Waals Complexes. Aniline−Ar_1 and −Ar_2 is a similar system in which we recently measured the binding energies.[2] The dissociation energy in An^+−Ar was measured to be 495 cm^{-1}. In that case we were also able to measure the energy required to remove both Ar atoms, which was 1020 cm^{-1}, establishing that the binding energy of the second Ar atom was 525 cm^{-1}, within experimental error the same as the binding energy of the first Ar atom. The An^+−Ar_2 system had an interesting twist in that the energy to remove the first Ar atom was quite low (380 cm^{-1}), establishing that there was in fact a lower energy conformation for the product An^+−Ar complex. This was postulated to be a hydrogen-bound geometry, which was not directly accessible from the π-bound neutral geometry. The results presented herein on BZD show that the energy required to remove one Ar atom from the $n = 2$ complex is very similar to the binding energy of the $n = 1$ complex and does not suggest a lower energy exit channel. This is useful information since ionization often leads to large changes in the intermolecular potential and the possibility for different structures in the cation which cannot be directly reached by photoexcitation from the cold neutral complex. Therefore, we are confident that the current measurements represent the dissociation energy from the global minimum on the cation surface.

The BZD complexes reported herein are structurally quite similar to the dibenzofuran and dibenzo-*p*-dioxin complexes measured by Grebner et al.[39] Measured binding energies for these and a number of other aromatic−Ar complexes are listed in Table 2. The result for the cation binding energy for BZD (625 cm^{-1}) is almost identical to that of dibenzofuran (636

cm^{-1}) but less than dibenzo-*p*-dioxin (739 cm^{-1}). This last result is particularly surprising given that dibenzo-*p*-dioxin is a two-ring system with the charge expected to be delocalized on both aromatic rings. One might have expected this to reduce the charge-induced dipole contribution to the cation complex binding energy, but in fact this three-ring system has a larger binding energy than the two-ring BZD system. Dibenzofuran is a three-ring system, but the central ring is five-membered with only one oxygen atom and so is not as close a comparison to BZD as dibenzo-*p*-dioxin.

The difference in the binding energies of BZD and dibenzo-*p*-dioxin is likely due to the difference in the neutral binding energies. For BZD, the neutral ground-state value is 417 cm^{-1}, whereas for dibenzo-*p*-dioxin it is 527 cm^{-1}. This difference of 110 cm^{-1} is almost exactly the difference of the cation binding energies. This further points out the fact that although the charge plays a significant role in the cation binding energy, the dispersive interactions are still dominant.

Summary

The electronic spectroscopy of BZD has been extended to measurements of the vibronic strucuture of the cation ground state using mass resolved threshold ionization spectroscopy. The ν_{25} and ν_{48} modes, which are prominent contributors to the S_1 spectra, are seen to have modest vibronic activity in the S_1 to cation spectrum. The ν_{25} twisting mode has a fundamental value of 146 cm^{-1}, which is intermediate between the ground-state and S_1 values. The ν_{48} bending mode is observed to increase in frequency in the cation to a value of 125 cm^{-1}, partly due to a strengthening of the C−O bonds in the cation.

The vibronic spectra of the BZD−Ar and BZD−Ar_2 complexes are measured in both the S_1 and cation ground states. Direct structural information is not obtained, but the similarity of the spectra to related systems and quantum chemical calculations indicate that Ar is bound to the π-system of the phenyl group. MATI dissociation spectra were used to determine the binding energy for the loss of one Ar atom from BZD^+−Ar and BZD^+−Ar_2. The binding energies were found to be quite large, 630 ± 10 and 650 ± 10 cm^{-1}, respectively, and quite similar to each other. The relatively sharp dissociation threshold for BZD^+−Ar_2 indicates that the translational energy release in the dissociation process is modest. The similar binding energies support the proposed structure of a sandwich-type complex in which both Ar atoms occupy almost identical binding sites on either side of the phenyl ring.

Acknowledgment. We gratefully acknowledge the computational resources provided on the Wesleyan University computer cluster supported by the NSF under Grant No. CNS-0619508.

References and Notes

(1) Yang, J.; Wagner, M.; Laane, J. *J. Phys. Chem. A* **2006**, *110*, 9805.
(2) Gu, Q.; Knee, J. L. *J. Chem. Phys.* **2008**, *128*, 064311.
(3) Burgi, T.; Droz, T.; Leutwyler, S. *Chem. Phys. Lett.* **1995**, *246*, 291.
(4) Droz, T.; Burgi, T.; Leutwyler, S. *J. Chem. Phys.* **1995**, *103*, 4035.
(5) Wickleder, C.; Henseler, D.; Leutwyler, S. *J. Chem. Phys.* **2002**, *116*, 1850.
(6) Bellm, S. M.; Lawrance, W. D. *Chem. Phys. Lett.* **2003**, *368*, 542.
(7) Nimlos, M. R.; Young, M. A.; Bernstein, E. R.; Kelley, D. F. *J. Chem. Phys.* **1989**, *91*, 5268.
(8) Lembach, G.; Brutschy, B. *J. Chem. Phys.* **1997**, *107*, 6156.
(9) Lembach, G.; Brutschy, B. *J. Phys. Chem. A* **1998**, *102*, 6068.
(10) Krause, H.; Neusser, H. J. *J. Chem. Phys.* **1992**, *97*, 5923.
(11) Krause, H.; Neusser, H. J. *J. Chem. Phys.* **1993**, *99*, 6278.
(12) Krause, H.; Neusser, H. J. *J. Photochem. Photobiol., A* **1994**, *80*, 73.
(13) Grebner, T. L.; Neusser, H. J. *Int. J. Mass Spectrom. Ion Processes* **1996**, *159*, 137.
(14) Piest, H.; von Helden, G.; Meijer, G. *J. Chem. Phys.* **1999**, *110*, 2010.
(15) Satink, R. G.; Piest, H.; von Helden, G.; Meijer, G. *J. Chem. Phys.* **1999**, *111*, 10750.
(16) Solca, N.; Dopfer, O. *Eur. Phys. J. D* **2002**, *20*, 469.
(17) Solca, N.; Dopfer, O. *Chem. Phys. Lett.* **2003**, *369*, 68.
(18) Zhu, L. C.; Johnson, P. *J. Chem. Phys.* **1991**, *94*, 5769.
(19) Neusser, H. J.; Krause, H. *Chem. Rev.* **1994**, *94*, 1829.
(20) Pitts, J. D.; Knee, J. L. *J. Chem. Phys.* **1998**, *108*, 9632.
(21) Zhang, X.; Pitts, J. D.; Nadarajah, R.; Knee, J. L. *J. Chem. Phys.* **1997**, *107*, 8239.
(22) Amirav, A.; Even, U.; Jortner, J. *J. Chem. Phys.* **1981**, *75*, 2489.
(23) Amirav, A.; Sonnenschein, M.; Jortner, J. *Chem. Phys.* **1984**, *88*, 199.
(24) Haynam, C. A.; Brumbaugh, D. V.; Levy, D. H. *J. Chem. Phys.* **1984**, *80*, 2256.
(25) Xu, Z.; Smith, J. M.; Knee, J. L. *J. Chem. Phys.* **1992**, *97*, 2843.
(26) Basu, S.; Knee, J. L. *J. Chem. Phys.* **2004**, *120*, 5631.
(27) Pitts, J. D.; Basu, S.; Knee, J. L. *J. Chem. Phys.* **2000**, *113*, 1857.
(28) Pitts, J. D.; Knee, J. L.; Wategaonkar, S. *J. Chem. Phys.* **1999**, *110*, 3378.
(29) Dietrich, H. J.; Lindner, R.; Muller-Dethlefs, K. *J. Chem. Phys.* **1994**, *101*, 3399.
(30) Wiley, W. C.; Mclaren, I. H. *Rev. Sci. Instrum.* **1955**, *26*, 1150.
(31) Smith, J. M.; Knee, J. L. *J. Chem. Phys.* **1993**, *99*, 38.
(32) Alvarez-Valtierra, L.; Pratt, D. W. *J. Chem. Phys.* **2007**, 126.
(33) Grebner, T. L.; von Unold, P.; Neusser, H. J. *J. Phys. Chem. A* **1997**, *101*, 158.
(34) Muller-Dethlefs, K.; Hobza, P. *Chem. Rev.* **2000**, *100*, 143.
(35) Makarewicz, J. *J. Chem. Phys.* **2004**, *121*, 8755.
(36) Cerny, J.; Tong, X.; Hobza, P.; Muller-Dethlefs, K. *J. Chem. Phys.* **2008**, 128.
(37) Dunning, T. H. *J. Phys. Chem. A* **2000**, *104*, 9062.
(38) Frisch, M. J.; Trucks, G. W.; Schlegel, H. B.; Scuseria, G. E.; Robb, M. A.; Cheeseman, J. R.; Montgomery, J. A., Jr.; Vreven, T.; Kudin, K. N.; Burant, J. C.; Millam, J. M.; Iyengar, S. S.; Tomasi, J.; Barone, V.; Mennucci, B.; Cossi, M.; Scalmani, G.; Rega, N.; Petersson, G. A.; Nakatsuji, H.; Hada, M.; Ehara, M.; Toyota, K.; Fukuda, R.; Hasegawa, J.; Ishida, M.; Nakajima, T.; Honda, Y.; Kitao, O.; Nakai, H.; Klene, M.; Li, X.; Knox, J. E.; Hratchian, H. P.; Cross, J. B.; Bakken, V.; Adamo, C.; Jaramillo, J.; Gomperts, R.; Stratmann, R. E.; Yazyev, O.; Austin, A. J.; Cammi, R.; Pomelli, C.; Ochterski, J. W.; Ayala, P. Y.; Morokuma, K.; Voth, G. A.; Salvador, P.; Dannenberg, J. J.; Zakrzewski, V. G.; Dapprich, S.; Daniels, A. D.; Strain, M. C.; Farkas, O.; Malick, D. K.; Rabuck, A. D.; Raghavachari, K.; Foresman, J. B.; Ortiz, J. V.; Cui, Q.; Baboul, A. G.; Clifford, S.; Cioslowski, J.; Stefanov, B. B.; Liu, G.; Liashenko, A.; Piskorz, P.; Komaromi, I.; Martin, R. L.; Fox, D. J.; Keith, T.; Al-Laham, M. A.; Peng, C. Y.; Nanayakkara, A.; Challacombe, M.; Gill, P. M. W.; Johnson, B.; Chen, W.; Wong, M. W.; Gonzalez, C.; Pople, J. A. *Gaussian 03*, revision C.02; Gaussian, Inc.: Wallingford, CT, 2004.
(39) Grebner, T. L.; Stumpf, R.; Neusser, H. J. *Int. J. Mass Spectrom.* **1997**, *167*, 649.
(40) Braun, J. E.; Grebner, T. L.; Neusser, H. J. *J. Phys. Chem. A* **1998**, *102*, 3273.
(41) Dessent, C. E. H.; Haines, S. R.; Muller-Dethlefs, K. *Chem. Phys. Lett.* **1999**, *315*, 103.

JP801716P